Chapter 9

Ribavirin triphosphate- and mismatch-stimulated 3′-to-5′ exonuclease activity of the SARS coronavirus RNA polymerase nsp12

Aartjan J.W. te Velthuis and Eric J. Snijder

Molecular Virology laboratory, Department of Medical Microbiology, Center of Infectious Diseases, Leiden University Medical Center, PO Box 9600, 2300RC Leiden, The Netherlands.

Abstract

Ribavirin is a purine analogue that can be efficiently incorporated into many viral RNA genomes. Once present, it induces the accumulation of transition mutations, which subsequently lead to error catastrophe and the inhibition of virus propagation. Furthermore, these effects may be more pronounced in larger viral RNA genomes. However, in spite of having RNA genomes that are ~3-fold larger than the typical RNA virus genome, the inhibitory effect of ribavirin on the replication of coronaviruses like SARS coronavirus (SARS-CoV) has been shown to be remarkably small. It was therefore hypothesised that CoVs may encode a rudimentary mechanism to prevent or correct misincorporation, and thus to avoid error catastrophe. Using *in vitro* assays and recombinant SARS-CoV nonstructural protein (nsp) 12, we show here that a 3′-to-5′ exonuclease activity is associated with this coronavirus polymerase. Importantly, this activity was stimulated by the presence of either ribavirin triphosphate (RTP) or an unpaired residue in the primer-template duplex, whereas mutations of RdRp motif B and residues in the nsp12 N-terminal domain altered these effects. Overall, these results lead us to suggest that SARS-CoV nsp12 may indeed be a viral RdRp that is capable of reducing its own error rate.

Introduction

The nucleoside ribavirin (1-β-D-ribofuranosyl-1,2,4-triazole-3-carboxamide) is a purine analogue that can enter cells as nucleotide precursor. Once converted to ribavirin triphosphate (RTP), it can be incorporated into RNA virus genomes by their cognate RNA-dependent RNA polymerases (RdRps) with efficiencies similar to those of ATP and GTP [180,276,320,321,426]. This property derives from the fact that ribavirin's carboxamide group can rotate and thereby alternate ribavirin's base pairing between uracil and cytosine. The consequence of this property is that ribavirin monophosphate (RMP) incorporated into the viral RNA can randomly induce transition mutations (G↔A; and C↔U in the opposite strand). In turn, this effect increases the overall mutation frequency of the virus and may thus rapidly result in an inhibition of viral replication and transcription[39,56,244,427,428,429]. Ribavirin is therefore a widely administered antiviral drug - alone or in combination with other compounds - for treatment of infections with viruses as diverse as Lassa virus, respiratory syncytial virus, and hepatitis C virus [92,93,94,95]. Furthermore, the analogue can effectively inhibit the replication of picornaviruses, orthomyxoviruses [96,97], hantaviruses [98,99], vaccinia virus [100], and reoviruses [101] in cell culture.

The sensitivity to ribavirin is highly variable among viruses, however. For example, to prevent plaque formation on Vero E6 cells, 1-25 μg/ml ribavirin is needed for the inhibition of the influenza A virus, while 25–100 μg/ml is required to inhibit HIV and other retroviruses [430]. Interestingly, to prevent cytopathology of severe acute respiratory syndrome coronavirus (SARS-CoV) on the same cell type, ribavirin concentrations of 0.5-5 mg/ml are required, a dose range that overlaps with the 50% cytotoxic dose (CD_{50}) for Vero E6 cell (generally ~0.2-1 mg/ml) [102,103,308,309]. Inhibiting concentrations close to the cytotoxic concentration (CC_{50}) of ribavirin on ST cells were also reported for two related swine CoVs, porcine respiratory CoV (PRCV) and transmissible gastroenteritis virus (TGEV) [431]. In line with these observations, ribavirin treatment of SARS-CoV-infected humans did not result in convincing antiviral effects during the 2003 outbreak [103], and similar findings were reported in mice infected with a mouse-adapted SARS-CoV strain [432].

With a nonsegmented, positive-stranded RNA (+RNA) genome of ~30 kb, approximately 3 fold larger than the average +RNA viral genome, SARS-CoV has one of the largest genomes among RNA viruses [58]. Theoretically, this unprecedented genome size should thus make it more sensitive to mutagen-induced error catastrophe, provided that we assume that the fidelity of the SARS-CoV replication and transcription complex (RTC) is similar to that of other RNA virus replicases. It has therefore been hypothesised that the surprisingly limited effect of ribavirin on CoV infections must be due to i) inefficient incorporation of RTP by one of the two SARS-CoV RdRps (*i.e.*, nonstructural proteins [nsps] 12 and 8) due to structural constraints in the nucleotide selection pocket

[89,154,156]; ii) negation of erroneous nucleotide incorporation through a correction mechanism involving a proofreading activity residing in one of the RdRps; iii) proofreading through a mechanism involving the nsp14 DEDD-type exonuclease [35,58], a viral enzyme whose inactivation was previously linked with the accumulation of viral mutations [105,106,107]; or iv) increased recombination rates between correct genome segments.

In light of the above hypotheses [35,89], we here document the observation that RTP and misaligned primer-template duplexes can stimulate a 3′-to-5′ exonuclease activity that is associated with the SARS-CoV RNA polymerase nsp12. Mutation of the polymerase motif B altered the efficiency of mismatch recognition, whereas single mutations in the unique N-terminal domain allowed us to impair exonuclease activity. These results thus lead us to suggest that SARS-CoV nsp12 possesses 3′-to-5′ exonuclease activity that is stimulated by an ability to recognise the nucleotide analogue RTP and errors in the template-primer duplex.

Results and discussion

SARS-CoV nsp12 has 3′-to-5′ exonuclease activity

Comparative sequence analysis has shown that the conserved, canonical RdRp domain of CoVs resides in the C-terminal two thirds of the 106-kDa nsp12 protein [274]. Subsequent biochemical studies have demonstrated the ability of this replicase subunit to incorporate nucleotides using both RNA and DNA templates [89,154]. Interestingly, during our analysis of the nsp12 primer-extension activity in the presence of ATP [154], we also noted a weak degradation of 5′ ^{32}P-labelled RNA oligos that was more pronounced in reactions containing the RdRp active site mutant D618A than in reactions containing wild-type nsp12. To investigate this activity in more detail and its significance in view of the hypothesised proofreading ability of CoV RdRps, we purified a recombinant SARS-CoV nsp12-RdRp as described previously [154] and incubated this enzyme with 5′ ^{32}P-labelled single-stranded DNA (ssDNA) and ssRNA oligonucleotides. Analysis of the reaction by 20% denaturing PAGE and autoradiography demonstrated that these nsp12 preparations were indeed able to slowly degrade both DNA and RNA (Fig. 1A and 1B). Interestingly, we previously observed that nsp12 has polymerase activity on both templates as well [154]. Given that the 5′ ^{32}P-labelled substrates were gradually hydrolysed to increasingly smaller labelled products, we conclude that this exonuclease activity has a 3′-to-5′ directionality.

Although the exonuclease activity for most optimal substrate for the exonuclease activity of DNA-dependent DNA polymerase (DdDps) is ssDNA, the physiologic relevant one is a primer-template duplex, whose primer strand must be melted in order to transfer the 3′-end of the primer to the exonuclease active site [54,433]. To study the

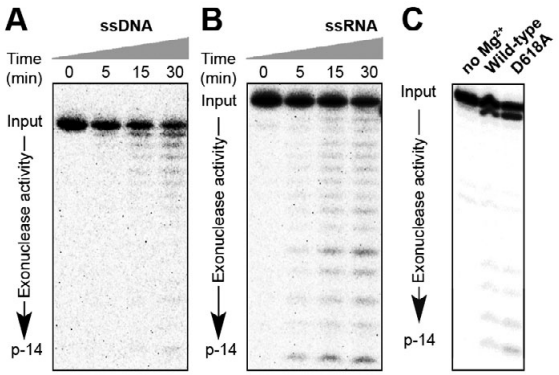

Figure 1. Nsp12 exonuclease activity has 3′-to-5′ directionality on both ssDNA and ssRNA templates. (**A**) To investigate the directionality of the SARS-CoV exonuclease activity, 5′^{32}P-labelled DNA or (**B**) RNA oligos were incubated in the presence of 6 mM Mg^{2+} and purified SARS-CoV nsp12. Samples were stopped at the indicated time points and resolved by 20% PAGE/7M urea gels. (**C**) SARS-CoV nsp12 is able to cleave a primer that was annealed to template RNA in the presence of 6 mM Mg^{2+}. A similar activity was observed for RdRp active site mutant D618A. Assays were stopped after 60 min and resolved with 20% PAGE/7M urea gels.

activity of nsp12 on such a template, we hybridised the 5′ ^{32}P-labelled RNA primer to a 40-mer template that was partially based on the 3′ untranslated region (UTR) of the SARS-CoV genome (residues 29512-29532) [154]. As shown in Fig. 1C, both nsp12 and the polymerase active site mutant D618A both degraded the primer in this 20-mer/40-mer primer-template configuration, albeit with very limited processivity. In absence of magnesium ions, no significant exonuclease activity was observed (Fig. 1C).

SARS-CoV nsp12 prefers magnesium ions for activity

To characterise the influence of divalent metal ions on the nsp12 exonuclease activity, we next substituted the optimal Mg^{2+} concentration for primer extension (6 mM; [154]) with different concentrations of Mg^{2+} or other divalent metals. As shown in Fig. S1, nsp12 was able to hydrolyse the 3′ end of ssRNAs under all Mg^{2+} concentrations and a low mM Mn^{2+} concentrations. The presence of Zn^{2+}, in line with its negative effects on the template binding affinity of SARS-CoV nsp12 [325], or high concentrations of Mn^{2+} significantly reduced nsp12′s exonuclease activity (Fig. S1).

Sequence analysis of the coronavirus nsp12 N-terminal domain identifies residues involved in exonuclease activity

Presently, the active site residues involved in the exonuclease and proofreading abilities of viral polymerases have only been identified in DNA virus polymerases [166,434]. Similar to the Klenow fragment, these polymerases employ a two-metal ion mechanism to bind an attacking hydroxide ion and stabilise the leaving 3′-OH group [54,168,435,436].

Typically the exonuclease domain is a ~150-amino acid structure in the DdDp N-terminus and dependent on motif I residues DxE, motif II residues $Nx_{2-4}F/YD$, and motif III residues Yx_3D for activity [54,169,433,434]. Metal ion coordination in this structure is performed by the invariant acidic amino acids in the three motifs, whereas the binding and positioning of the single stranded part of the melded nascent strand requires the strictly conserved asparagine and aromatic residues (*i.e.*, Phe or Tyr) [54,169,433]. Using these well-characterised motifs as reference, we scanned the nsp12 sequence for putative exonuclease active site residues and identified a set of conserved aspartic acid and asparagine motifs positioned within ~120 amino acids of each other. As shown in Fig. 2A, these residues are spaced according to conserved Dx_2EN, DNx_2Dx_5YD and Dx_3YD motifs and reside in the N-terminal domain, a domain that is unique for CoVs and presently without assigned enzymatic function [58,89].

To investigate the involvement of the N-terminal domain in nsp12's ability to degrade an annealed RNA primer, we engineered three alanine substitutions in the most conserved N-terminal nsp12 motif (*i.e.*, motif II), targeting asparagine-209, aspartate-211 and apartate-218 (*i.e.*, N209, D211 and D218). All mutants were purified side-by-side using the same expression and purification protocol [154]. When we next examined the ability of these three mutants to degrade 5′ ^{32}P-labelled RNA, we found that the exonuclease activity of N209A was impaired by ~50% compared to the wild-type protein, whereas D211A and D218A demonstrated ~86% and ~72% reduced exonuclease activities, respectively (Fig. 2B and C).

To test the impact of the mutations on the basic polymerase activity of nsp12, we assessed their ability to extend the 20-nt primer used above as readout for the exonuclease assay through the incorporation of ATP and GTP, as described previously [154]. As shown in Fig. 2D and 2E, all mutations had less than wild-type primer extension activity on this template, suggesting that the C-terminal polymerase domain and the N-terminal domain are tightly integrated into the nsp12 structure. Such an integration of the two active sites and a correspondingly reciprocal effect of exonuclease active site mutations has also been observed for a number of viral DdDps [434,435].

An unpaired residue in the primer-template duplex stimulates SARS-CoV nsp12's 3′-to-5′ exonuclease activity.

Together the results presented in Fig. 1 and 2 suggested that nsp12 is able to hydrolyse RNA molecules with a 3′-to-5′ polarity and that this activity involves residues in the N-terminal domain. To investigate the significance of this activity for the proposed proofreading hypothesis, we incubated nsp12 with a primer-template duplex containing an unpaired residue at position -6-8 of the primer (Fig. 3A, primer 446). As was argued previously for DdDps [436], the recognition of such internally mismatched residues critically is important for the overall fidelity of the polymerase reaction, as they can then induce a

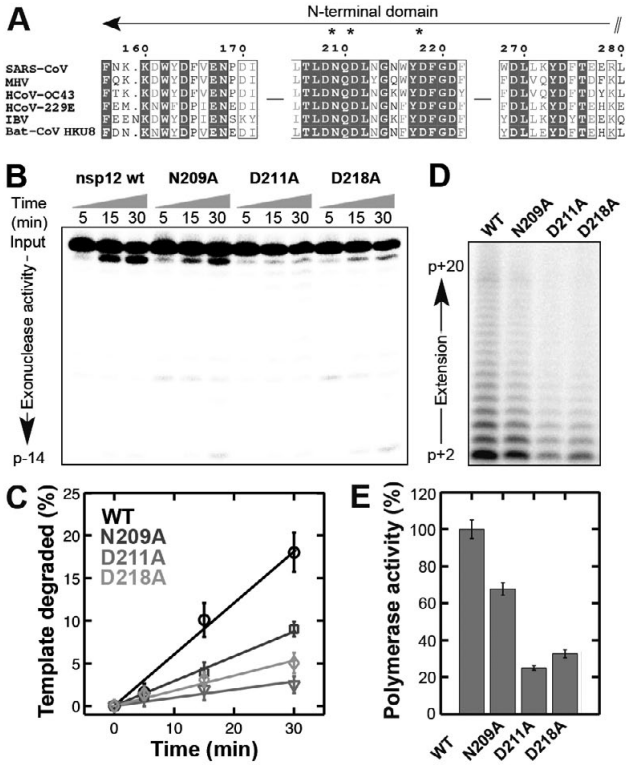

Figure 2. Conserved residues in the coronavirus nsp12 N-terminal domain influence exonuclease and RdRp activity. (**A**) Partial alignment of the N-terminal domain of CoV nsp12. Fully conserved residues are shaded dark grey, while partially conserved residues are boxed. The residues targeted by mutagenesis are indicated with asterisks. Mutants of aspartic acid and asparagine residues were chosen based on their conservation among CoV nsp12 proteins and their relatively similar spacing compared to the exonuclease domains of viral DNA polymerases. (**B**) Analysis of the effect of N-terminal domain mutations on SARS-CoV nsp12's ability to degrade a 5' ^{32}P-labelled primer in a dsRNA substrate. (**C**) Quantitation of the exonuclease activity. Percentages of degraded input RNA were plotted as function of time and fitted with a single polynomial. Error bars present standard deviation. (**D**) Analysis of the primer extension activity of wild-type SARS-CoV nsp12 and the nsp12 mutants on a heteromeric template. (**E**) Quantitation of the primer extension activity of SARS-CoV nsp12 mutants expressed as percentage of activity of the wild-type protein. Error bars represent standard deviations (n = 3).

global conformational change in the polymerase ground-state, which stalls polymerisation and allows the single stranded nascent strand to travel to the exonuclease site for mismatch removal. Indeed, when we incubated wild-type nsp12 with the misaligned template, we found that the exonuclease activity increased relative to the fully Watson-Crick base-paired template (Fig. 3B, left panel). In contrast, no significant stimulation of exonuclease activity was observed for mutant D218 in line with our observations in Fig. 2.

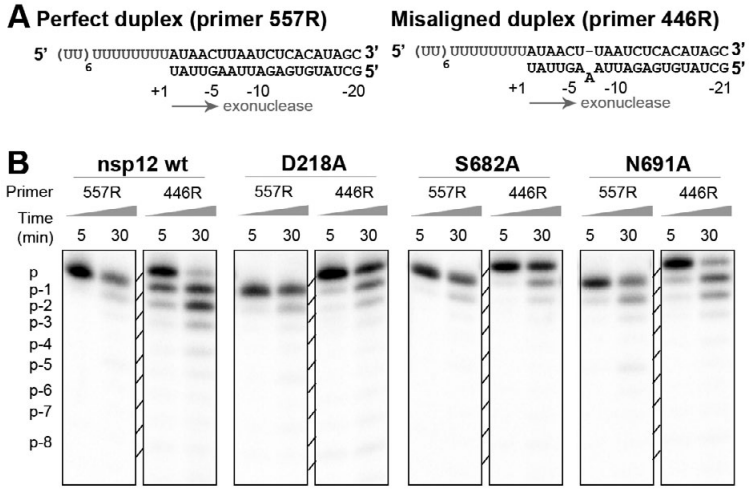

Figure 3. The 3′-to-5′ exonuclease activity of SARS-CoV nsp12 mutants is stimulated by mutation of conserved residues in nsp12. (**A**) To study the sensitivity of the nsp12 exonuclease activity to misalignments in the primer-template duplex, two templates were used. The first consisted of a perfect primer-duplex (primer 557), while the second used a primer (primer 446) with an additional adenosine, thus creating a primer-duplex containing an non-Watson-Crick paired residue at position -6 of the primer. (**B**) Wild type nsp12 and mutants D218A, S687A and N691A were incubated with 5′ ^{32}P-labelled primers hybridised to the template. Samples were taken after 5 and 30 minutes and resolved with 20% PAGE/7M urea gels.

In the RdRp structure, motif B residues are generally involved in nucleotide selection and the recognition of the primer-template duplex [89,132]. To explore the involvement of nsp12's motif B residues in exonuclease stimulation, we performed the above assay with nsp12 mutants containing alanine substitutions at the strictly conserved positions serine-682 and asparagine-691 (*i.e.*, S682 and N691; Fig. S1). As shown in Fig. 3C, we observed that mutation S682A failed to degrade the two templates with a significant difference, suggesting that this residue may be involved in the contact formation between the RdRp and the primer-template duplex. Mutant N691A on the other hand, was effectively stimulated by the presence of the mutation and degraded both primers with similar efficiency as the wild-type enzyme.

Ribavirin triphosphate stimulates exonuclease and re-incorporation activity

As was noted above, the commonly used antiviral drug and nucleotide analogue ribavirin has been deemed relatively ineffective against SARS-CoV infections [103,432]. One hypothesis to explain this phenomenon suggests that one or both of the SARS-CoV RdRps may be able to select against RTP incorporation or remove RMP moieties from the nascent strand [89,156]. To analyse the relevance of the observed SARS-CoV nsp12 exonuclease activity for RTP incorporation, we next incubated wild-type and mutant

nsp12 enzymes with either ATP or RTP and tested their ability to extend a 20-nt primer under these conditions. To ensure that only singe extension cycles could be performed, the RdRp assays were done in the presence of sufficient heparin to trap unbound polymerases (Fig. 4A). As outlined in Fig. 4, complex formation and 3′-labelling of the primer was achieved by incubating nsp12 with the partly double-stranded RNA template and a limiting concentration of [α-^{32}P]ATP (Fig. 4B, grey A residue). Next, heparin was added in addition to a 300-fold excess of non-radioactive ATP or RTP to facilitate further elongation of the primer (Fig. 4B).

As shown in Fig. 4C, the reference lane of wild-type nsp12, which had not been stimulated by addition of ATP or RTP, yielded the expected 3′-radiolabelled primer (indicated as 'p+1') as well as a minor product that was equal to the primer length (labelled 'p') (Fig. 4C, leftmost lane). This radioactive pattern suggested that a small fraction of the wild-type nsp12 had first hydrolysed the 3′ end of the primer and subsequently extended it by one nucleotide using the only available substrate in the reaction (*i.e.*, [α-^{32}P]ATP) before becoming inactive (Fig. 4C, Fig. S2). We observed significantly less p product in reactions containing nsp12 mutants D211A and S682A (Fig. 4C), in line with their reduced ability to attack the 3′ terminal residue of the primer in the exonuclease assays.

In the reactions containing wild-type nsp12, the subsequent addition of an excess of unlabelled ATP resulted in a distributive extension of the primer up to a dominant p+18 product (Fig. 4C and 4D), which is in line with previous observations [154]. A more detailed analysis of the lane profiles confirmed that the spacing between the p, p+1 and p+2 signals was identical and that the primer signal must have been the result of an ATP incorporation event (Fig. 4D). No decrease in the p signal was observed upon addition of an excess of unlabelled ATP, suggesting that the RdRps responsible for this product had indeed either dissociated from the template or had become inactive. In addition, this approach allowed us to verify that the p product in the D211A-reaction was indeed significantly reduced (Fig. 4E).

In contrast to the ATP reactions, the addition of RTP predominantly resulted in an increase of the p and p+1 signals (Fig. 4C). This was particularly evident in the lane profile analysis, in which the p+1 signal at pixel position 1075 showed a dramatic increase over the p+1 peak in the ATP reaction. Strikingly, a weak band corresponding to a p-1 signal, *i.e.* a product that was shorter than the original RNA primer, was observed as well (Fig. 4C, lower panel), suggesting that the RTP had stimulated the 3′ attack of the primer and (re)incorporation of the still present [α-^{32}P]ATP. Lane profile analysis confirmed that ATP had indeed been incorporated in all these three peaks, whereas RTP had clearly been used for incorporation in the p+2 product, as was evident from the migration shift of these bands (Fig. 4D). This result is in line with the 23.2 g/mol molecular weight (MW) difference between adenosine and ribavirin (MW_{ATP} = 507.2 g/mol; MW_{RTP} = 484.0 g/mol).

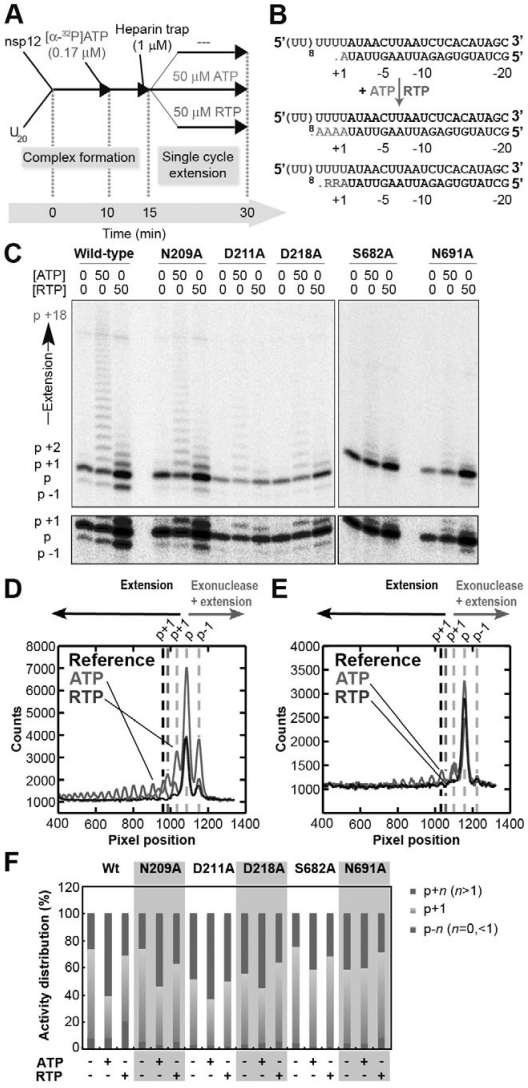

Figure 4. Interplay between the SARS-CoV nsp12 polymerase and exonuclease activities. (**A**) Schematic of nsp12 primer-extension experiments. Recombinant SARS-CoV nsp12 was first preincubated with an unlabelled primer-template complex and a low concentration of [α-^{32}P]ATP to establish complex formation and 3′ radiolabelling of the primer. Heparin was subsequently added to a final concentration of 1 μM to trap free polymerase before reactions were split in 3 aliquots. To allow extension, 50 μM non-radioactive ATP or RTP was then added to two of these samples, followed by a 30-min incubation. (**B**) Overview of expected radiolabelled products on the provided template assuming that nsp12 only has polymerase activity. (**C**) Activity of SARS-CoV nsp12 in the presence of an excess of ATP or RTP. For wild-type nsp12, elevated p-1, primer and p+1 signals are evident in the presence of RTP relative to reactions performed in the presence of ATP. Interestingly, this behaviour changed upon mutation of conserved nsp12 residues to alanine, most notably through mutation D211A. Samples were resolved with 20% PAGE/7M urea gels. The lower

Figure 4 continued
panel is a longer exposure of the upper panel. (**D**) Lane profile analysis can be used to distinguish between the incorporation of ATP and RTP in the ATP- and RTP-containing lanes given their different migration in the 20% PAGE gels. These differences are only visible for the p+2 and longer products (compare black dashed line [ATP] with dark grey dashed line [RTP]), whereas the p and p-1 products are all separated with an AMP-like interval (light grey dashed lines), suggesting that they result from hydrolysis of the 3′ terminal nucleotide of the primer and the (mis)incorporation of [α-^{32}P]ATP. (**E**) The p and p-1 products are significantly reduced compared to the reference signalin mutant D211A. (**F**) Normalised distributions of the SARS-CoV nsp12 polymerase activity.

To obtain a better estimate of the effects of ATP and RTP on the overall polymerase reaction, we calculated the normalised distribution of the primer extension signal (all products longer than p+1, *i.e.*, p+n with n>1), the initial 3′ labelling (p+1), and all products that were shorter than any extension of the primer (p+n with n=0 or n<1). As shown in Fig. 4F, this analysis supported our previous conclusions and showed that only the wild-type nsp12 and mutant N691 displayed a >2 fold increase of the activity that required RTP-induced exonuclease active site and a reincorporation of [α-^{32}P]ATP (Fig. 4F and Fig. S2). This signal was reduced in all other mutants, in line the significantly impaired exonuclease activity of the N-terminal domain mutants, and mutant S682A's inability to stimulate exonuclease activity in the presence of a template-primer mismatch. Interestingly, all extension signals were affected by the presence of RTP (Fig. 4F), suggesting that nsp12 is able to discriminate between the ATP and RTP, but that none of the residues targeted by our mutagenesis is essential for this discrimination during incorporation.

Concluding remarks

With genomes of ~30 kb, CoVs are a unique family of +RNA viruses that have evolved the largest nonsegmented RNA genomes known to date. In addition to genome replication, expression of these giant genomes requires the synthesis of subgenomic (sg) mRNAs, which have a common leader sequence at their 5′ end and an identical 3′-terminal segment [323]. Current evidence suggests that these products are formed during a process that starts with discontinuous minus-strand RNA (-RNA) synthesis and produces a nested set of sg-length -RNAs that can be used as template for the production of the sg mRNAs [51,266,416]. It is believed that as CoVs evolved these features, genome expansion and the development of a more complex enzymology than other +RNA viruses went hand in hand. To minimise the number of mutations per replicated genome, these enzymes likely included proteins capable of performing RNA-based proofreading or some other form of error prevention [35,58,323,437]. Interestingly, previous deep-sequencing analysis of the progeny of a SARS-CoV mutant containing an inactivated nsp14 exonuclease domain did indeed demonstrate a significantly increased mutation frequency compared to the-wild type control [106,107]. This virus mutant was therefore denoted as "infidelity

mutant" and nsp14 was proposed to be a key component of a putative coronavirus proofreading mechanism. A direct observation of mutation-recognition by nsp14 has so far not been made, however, and mechanistic information about its possible mode of action in the viral RTC is still lacking.

Interesting in the light of the proposed proofreading hypothesis, we here describe that the SARS-CoV polymerase nsp12 has 3′-to-5′ exonuclease activity as well. Furthermore, guided by the well-established of the DdDp exonuclease active site and a model structure based on comparative sequence analysis between the C-terminal two-thirds of SARS-CoV nsp12 and many well-studied RdRps [89,166,434], we were able to engineer nsp12 mutants that could alter its exonuclease activity (Fig. 2) and its ability to recognise primer-template mismatches (Fig. 3). Together, these observations lead us to suggest that one of the SARS-CoV RdRps has a proofreading ability that is tightly interwoven with its polymerase function. It will be of importance to investigate the involvement of nsp12 in the proposed CoV proofreading mechanism and to test whether it may function in conjunction with the multifunctional exonuclease-methyltransfase enzyme nsp14 [105,107].

Materials and methods

SARS-CoV nsp12 purification and mutagenesis

All proteins used were expressed and purified as described previously [154]. The nsp12 mutants listed in Table S1 were engineered in the pASK3-Ub-nsp12-CHis$_6$ expression vector [154] via site-directed mutagenesis according to the QuikChange protocol (Stratagene) and the in Table S1 listed primers.

Polymerase and exonuclease experiments

The oligoribonucleotide substrates used for polymerase assays indicated in Fig. 2 and 4 were prepared as described previously [154]. Primer-extension assays were essentially performed as described elsewhere [154], using 50 μM ATP (Roche) or RTP (Jena Bioscience) for extension. For exonuclease assays, 0.25 μM of purified nsp12 was typically incubated with 1 nM of 5′ ^{32}P-labelled ssDNA, ssRNA or duplex RNA and 6 mM Mg^{2+} at 20 °C. Reaction times are indicated in the figures, while all reaction buffers contained 1mM DTT, 0.1% Triton X-100, 10 mM KCl, 10 mM NaCl, 5% glycerol and 20 mM Tris (pH 8.0). Gels were dried on Whatman filter paper and bands were quantified by phosphorimaging using a Typhoon variable mode scanner (GE Healthcare) and ImageQuant TL 7.0 software (GE Healthcare). Lane profile densities were exported from ImageQuant TL 7.0 and aligned by the p+1 density using Matlab 2009a.

Sequence alignment

Alignments of nsp12 sequences were made using Muscle [327]. Sequences used included the alphacoronaviruses human CoV 229E (NC_002645); the betacoronaviruses SARS-CoV Frankfurt-1 (AY291315), mouse hepatitis virus A59 (MHV, NC_001849), and human CoV OC43 (NC_005147); and the gammacoronavirus avian infectious bronchitis virus (IBV, AJ311317).

Acknowledgements

We thank Dr Alexander Gorbalenya, Dr Craig Cameron, and Dr Clara Posthuma for stimulating discussions. This work was supported by the Netherlands Organization for Scientific Research (NWO) through Toptalent grant (021.001.037), a grant from the Council for Chemical Sciences (700.55.002), and the European Union Seventh Framework Programme (FP7/2007-2013) under SILVER grant agreement n° 260644.

CHAPTER 9 - SUPPLEMENTAL INFORMATION

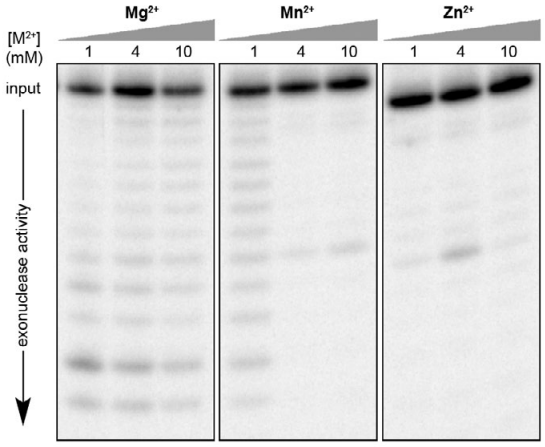

Figure S1: Influence of divalent metal ions on the SARS-CoV nsp12 activity. Wild-type nsp12 was incubated with different concentrations of Mg^{2+}, Mn^{2+} and Zn^{2+} and assessed for its ability to degrade a 5′ ^{32}P-labelled ssRNA under these conditions. Samples were resolved by 20%/7M Urea PAGE after 60 min.

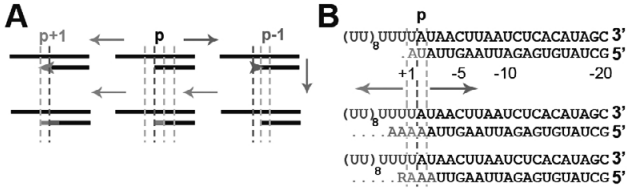

Figure S2: Schematic presentation of interplay between the SARS-CoV nsp12 primer-extension and exonuclease activities. (**A**) In the presence of low concentrations of [α-^{32}P]ATP, wild type SARS-CoV nsp12 can extend the 3′ end of the primer (short black line) with a radioactively labelled AMP (indicated in light grey), but also perform a 3′→5′ digestion-extension reaction (indicated in dark grey). Given that only [α-^{32}P]AMP was provided during the preincubation, this can result in the synthesis of p and p+1 products through the incorporation of [α-^{32}P]AMP and thus two radioactive products. (**B**) Effectively the radiolabelling of p is a misincorporation (indicated as grey A) and thus results in the replacement of the 3′ U with a [α-^{32}P]AMP in a small population of the templates. When an excess of ATP is subsequently added, further extension of the primer can be observed (indicated with green A residues). In the presence of RTP, however, the frequency of the 3′ exonuclease-extension reactions increases, which results in [α-^{32}P]AMP-labelling of the p-1 position.

Table S1: primers for nsp12 mutagenesis

Mutant	Primer	Sequence (5′-to-3′)
N209A	SAV547	GTACTGACATTAGATGCTCAGGATCTTAATGGG
	SAV548	CCCATTAAGATCCTGAGCATCTAATGTCAGTAC
D211A	SAV549	ACATTAGATAATCAGGCTCTTAATGGGAACTGG
	SAV550	CCAGTTCCCATTAAGAGCCTGATTATCTAATGA
D218A	SAV551	AATGGGAACTGGTACGCTTTCGGTGATTTCGTA
	SAV552	TACGAAATCACCGAAAGCGTACCAGTTCCCATT
S682A	SAV618	CAGGTGGAACATCAGCCCGGTGATGCTACAACT
	SAV619	AGTTGTAGCATCACCGGCTGATGTTCCACCTG
N691A	SAV622	ACAACTGCTTATGCTGCTAGTGTCTTTAACATT
	SAV623	AATGTTAAAGACACTAGCAGCATAAGCAGTTGT
S795A	SAV626	AATAATGTGTTCATGGCTGAGGCAAAATGTTGG
	SAV627	CCAACATTTTGCCTCAGCCATGAACACATTATT